ACS Macro Letters

Letter

pubs.acs.org/macroletters

Relaxation in Thin Polymer Films Mapped across the Film Thickness by Astigmatic Single-Molecule Imaging

Tatsuya Oba and Martin Vacha*

Department of Organic and Polymeric Materials, Tokyo Institute of Technology, Ookayama 2-12-1-S8, Meguro-ku, Tokyo 152-8552, Japan

Supporting Information

ABSTRACT: We have studied relaxation processes in thin supported films of poly(methyl acrylate) at the temperature corresponding to 13 K above the glass transition by monitoring the reorientation of single perylenediimide molecules doped into the films. The axial position of the dye molecules across the thickness of the film was determined with a resolution of 12 nm by analyzing astigmatic fluorescence images. The average relaxation times of the rotating molecules do not depend on the overall thickness of the film between 20 and 110 nm. The relaxation times also do not show any dependence on the axial position within the films for the film thickness between 70 and 110 nm. In addition to the rotating molecules we observed a fraction of spatially diffusing molecules and completely immobile molecules. These molecules indicate the presence of thin (<5 nm) high-mobility surface layer and low-mobility layer at the interface with the substrate.

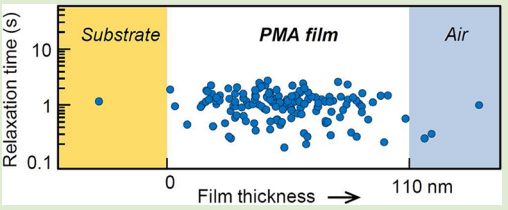

Polymers show different physical properties when their physical dimensions are reduced from bulk to the nanoscale level. Such changes are of interest both from the point of basic polymer physics and from the point of technological applications. One of the parameters that changes upon downscaling is the glass transition temperature (T_g) and the related polymer relaxation processes. Interest in this phenomenon has been spurred by the observation by ellipsometry that T_g in thin supported film of polystyrene (PS) decreases together with decreasing film thickness.[1] Other experiments by different groups confirmed deviation from bulk T_g in supported and free-standing polymer thin films.[2−6] The trend in the T_g can be both decreasing as a result of the prevailing effect of free surface or increasing if the interaction on the interface with the substrate is dominant. The effect of the free surface has been described in terms of a liquid-like layer in which the polymer chains have higher mobility compared to the film interior and the thickness of which increases with increasing temperature.[2,7,8] Detailed studies on the T_g profile in supported and free-standing PS and other films showed that there is a gradient of the enhanced mobility extending from the surface into the film and that the length scale of the surface effect is on the order of tens of nanometers.[9−11] The continuous change from the fast relaxation at the surface into the bulk-like dynamics within the film has been also reproduced by molecular dynamics simulations.[12] On the other hand, there are studies that do not support the above picture. A much thinner (<7 nm) high mobility layer at T_g in free-standing PS films has been found independent of the total film thickness.[13] Other methods did not find evidence of T_g deviation larger than 3 K in a wide range of the film thickness.[14,15]

One of the main difficulties in studying the effect of the surface in thin polymer films is that most of the methods probe the film as a whole without quantifying and controlling the studied position with respect to the surface. Even methods that do have some extent of resolution along the film thickness either probe only the topmost layer (<3 nm) such as the scanning force microscopic techniques,[16] or their resolution is limited by the minimum thickness of a labeled intermediate layers in multilayer composite films.[9−11] A method that has in the past 20 years attracted attention because of its ability to remove spatial and temporal averaging is single molecule spectroscopy (SMS). As such, SMS is an ideal tool for the study of highly heterogeneous systems such as glasses, amorphous polymers, and other types of soft matter.[17−19] Examples from the fields of synthetic polymers include the diffusion of labeled polymers[20] or small molecular probes[21] in an unlabeled polymer matrix, studies of glass and polymer relaxation processes near T_g by monitoring molecular probe reorientation,[22−30] or the study of polymer segmental motion by detecting changes in a single probe molecule fluorescence lifetime.[31] These studies have confirmed the existence of dynamic heterogeneities in relaxation of glass forming solids and indicated lateral spatial heterogeneities on scales of the order of optical resolution.

In this study, we employ a recently demonstrated SMS technique[32] that uses controlled astigmatism in the detection path of single-molecule fluorescence to determine axial position of the probe molecule along the thickness of polymer film. Compared to the diffraction-limited focal depth of conventional fluorescence microscopy which is on the order of hundreds of nanometers, astigmatic imaging provides axial resolution beyond the diffraction limit[33] and has been successfully used,

Received: May 8, 2012
Accepted: June 6, 2012
Published: June 8, 2012

   dx.doi.org/10.1021/mz3002269 | ACS Macro Lett. 2012, 1, 784−788

for example, to image specific proteins inside live bacterial cells.[34] In our experiments, the astigmatism is combined with polarization detection which enables to monitor rotational motion of the probe molecules via the measurement of fluorescence linear dichroism. We use the technique to study position-dependent relaxation dynamics in supported films of poly(methyl acrylate) with thickness ranging from 20 to 110 nm.

Samples were prepared by spin-coating toluene solution of poly(methyl acrylate) (PMA, Aldrich, M_w = 40 000 g/mol, T_g = 281 K) on cleaned coverslips to achieve film thicknesses of 20, 70, and 110 nm. The polymer solution has been doped with the dye *N*,N_0-dioctyl-3,4,9,10-perylenedicarboximide (PDI, Aldrich) at the concentration of 1×10^{-11} M to 1×10^{-12} M. The films were dried in a vacuum oven for 3 h and used immediately for experiments.

The scheme of the experimental setup which is based on an inverted fluorescence microscope (Olympus IX71) is shown in Figure 1a. The fluorescence is excited by a circularly polarized

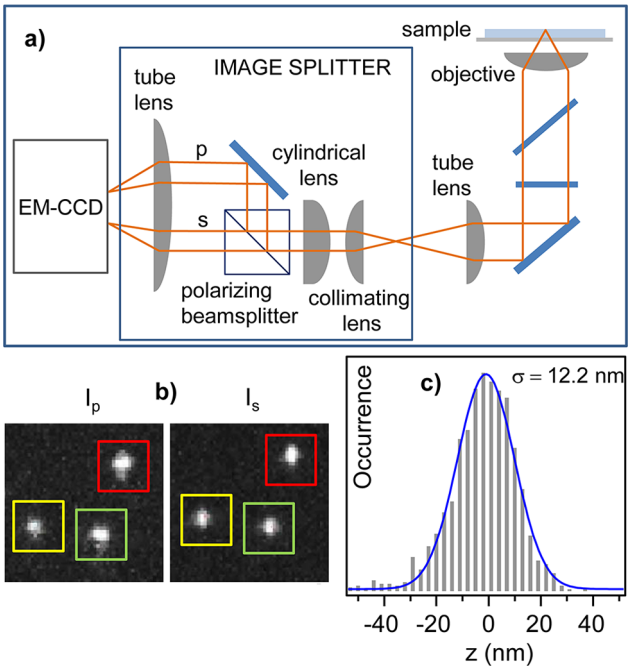

Figure 1. (a) Scheme of the experimental setup; (b) typical single-molecule astigmatic images taken in the two orthogonal polarization detection channels; (c) histogram of the *z*-position determined by averaging 10 consecutive positions for each molecule.

488 nm laser line of an Ar−Kr ion laser and collected using an oil-immersion lens (Olympus UPlanFLN100XO2, 100×, NA = 1.3). The astigmatism is introduced in the detection path by inserting a cylindrical lens (focal length 500 mm) in an image splitter (Optosplit II, Cairn Research) placed at the side port of the microscope. The image is split by wire-grid polarizing beamsplitter into two orthogonal polarization paths which are reimaged onto an electron multiplication charge-coupled device (CCD) camera (Andor, iXon+).

In typical experiments 2500 consecutive CCD camera images are recorded with an integration time of 200 ms per frame. An example of the two orthogonal polarization images taken with the cylindrical lens are shown in Figure 1b. The astigmatic images were analyzed by fitting with asymmetric two-dimensional Gaussian functions. The fitting provides a ratio of the two dimensions of the elongated image of a single PDI molecule. The position of a particular molecule along the *z*-axis (perpendicular to the sample plane) is obtained by comparing this ratio value with a calibration curve. Details of the experimental procedure can be found in the Supporting Information. The position accuracy along the *z*-axis was evaluated by plotting a histogram of *z*-positions of a large ensemble of molecules, each taken as an average position obtained from 10 consecutive images. The histogram (shown in Figure 1c) is well fit with a Gaussian distribution with a standard deviation of 12.2 nm which can be taken as a measure of the *z*-axis resolution.

A majority of the PDI molecules studied showed dynamic behavior due to reorientation (rotation) in the polymer matrix. The reorientation is analyzed by plotting fluorescence intensity time traces for both orthogonal polarizations $I_p(t)$ and $I_s(t)$ for each molecule. An example of such traces is shown in Figure 2a.

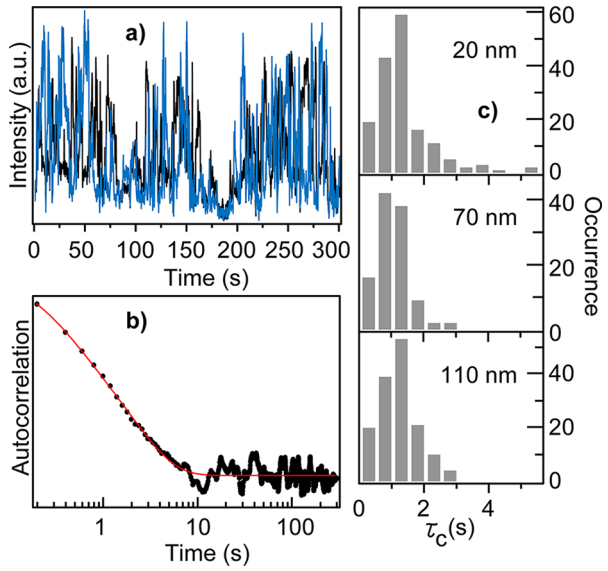

Figure 2. (a) Typical fluorescence intensity time traces of a single molecule; black, *s*-polarization; blue, *p*-polarization; (b) example of a linear dichroism autocorrelation function (black symbols) fitted with the KWW stretched exponential (red); (c) Histograms of the average relaxation times τ_c obtained for the (from top to bottom) 20 nm, 70 and 110 nm films.

As expected, the two intensity traces are anticorrelated except for periods of fluorescence blinking. The traces of each molecule were further used to calculate the fluorescence linear dichroism $A(t)$ as

$$A(t) = \frac{I_p(t) - I_s(t)}{I_p(t) + I_s(t)} \quad (1)$$

and the linear dichroism autocorrelation function $C(\tau) = \langle A(t)A(t+\tau)\rangle / \langle A(t)A(t)\rangle$, an example of which is presented in Figure 2b. The autocorrelation function was then fit with the Kohlrausch−Williams−Watt (KWW) stretched exponential

$$C(\tau) = C_1 \exp(-\tau/\tau_s)^{\beta} \quad (2)$$

in which C_1 is a coefficient, τ_s is the relaxation time, and the parameter β is related to the inhomogeneity of the relaxation process. The fitting parameters τ_s and β obtained for each

dx.doi.org/10.1021/mz3002269 | ACS Macro Lett. 2012, 1, 784−788

molecule were used to calculate the average relaxation time τ_c as

$$\tau_c = \frac{\tau_s}{\beta}\Gamma\left(\frac{1}{\beta}\right) \quad (3)$$

where Γ is a gamma function.

The average relaxation times τ_c obtained in the PMA films of different thickness are summarized in histograms in Figure 2c. The obtained values of the β coefficients show distributions with peaks between 0.6 and 0.8. The distributions are presented in the Supporting Information. Independent of the thickness the three films show very similar distributions of the relaxation times, with mean values (calculated as means of the distributions) of 1.41 s for the 20 nm film, 1.28 s for the 70 nm film, and 1.12 s for the 110 nm film. The slightly larger mean value of the 20 nm film is due to the presence of the long tail of the distribution toward longer relaxation times. Overall, however, the mean times are in very good agreement with those reported for other PMA films.[24,25]

The relaxation times τ_c are shown as a function of the z-position of the molecules within the film in the Figure 3a. Since

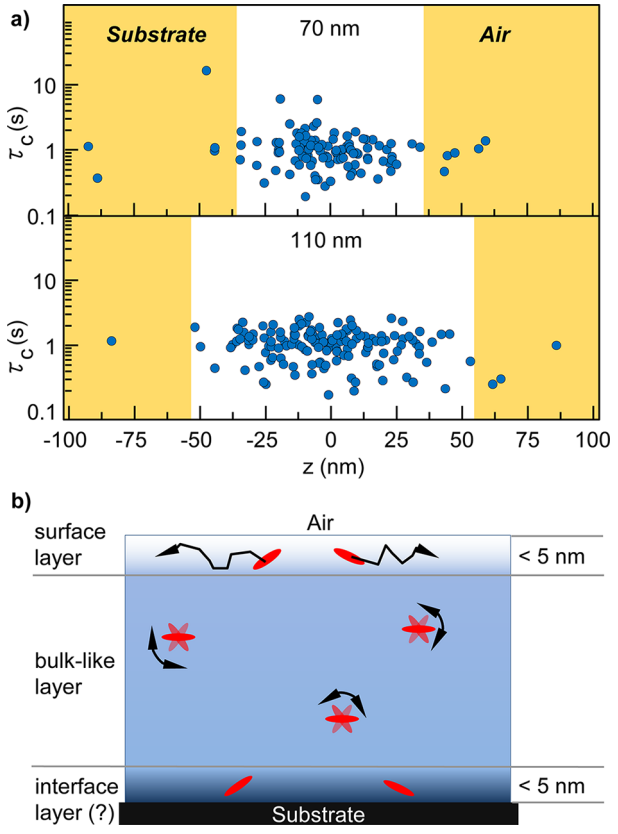

Figure 3. (a) Average relaxation times τ_c plotted as a function of the z-position of the molecule within the film for the 70 nm film (top) and the 110 nm film (bottom); (b) schematic proposal of the structure of the supported thin PMA film.

the z-resolution is comparable to the thickness of the 20 nm film, only data for the 70 and 110 nm films are plotted in the figure. The color shaded areas represent the position of the substrate and air, respectively. The reliability of the z-position determination is supported by the fact that only 9% of the total of 112 molecules in the 70 nm film and 5% of the 145 molecules in the 110 nm film are found outside of the film z-position range (i.e., either in the substrate or in the air). The fact that some of the molecules are displaced by a large amount from the area of the film is a consequence of the normal distribution of the z-position determination as shown in Figure 1c. It is apparent from the Figure 3a that there is no obvious trend in the values of the relaxation time along the thickness of the sample and the times are evenly distributed across the film.

As mentioned above, reorienting (rotating) PDI molecules represent the majority of the observed single molecules. However, apart from these there is also a fraction of molecules in each film which show changes of position with time. An example of such spatially diffusing molecule is shown in Figure 4. The fraction of the diffusing molecules depends on the film

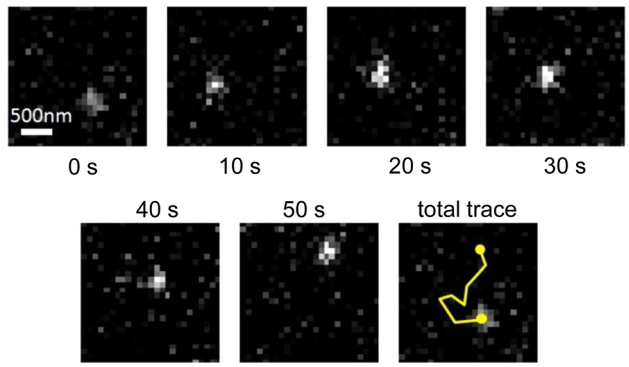

Figure 4. Spatial positions of a diffusing molecule at different detection times and the total diffusion trace (yellow line).

thickness and decreases from 0.17 for the 20 nm film to 0.02 for the 110 nm film. The fact that the molecules are diffusing does not allow reliable determination of their z-position. We may, however, assume that these molecules are located in the surface layer with higher chain mobility. Further, assuming that all PDI molecules are dispersed homogeneously in the film, we can estimate the thickness of the surface layer between 2 and 4 nm. Given the large error it is more meaningful to estimate the surface layer thickness at <5 nm, independent of the film thickness. It has been shown before that the onset of translation motion for single molecules in PMA films is approximately at $1.2T_g$.[24] This result allows us to estimate that the high-mobility surface layer finds itself at an effective temperature of T_g + 50 K.

Apart from the rotating and diffusing molecules we also observed a very small fraction of molecules that do not exhibit any dynamic behavior within the time interval of the measurement. In these molecules the specific emission pattern of a single dipole emitter is not averaged as in the case of rotating molecules, and this pattern introduces further inaccuracy in determining its z-position. The only information that we were able to obtain from the position determination of these immobile molecules is that they tend to be located more toward the interface with the substrate. In analogy with the surface layer, we may assume the existence of an interface layer characterized by lower mobility, the thickness of which would be <5 nm. The assumption of the lower mobility layer is supported by the fact that in the 20 nm film we have found (next to the immobile molecules) also the relatively largest fraction of molecules with longer relaxation times, as seen in the long tail of the distribution in Figure 2c.

To summarize the experimental observations, we measured relaxation times of single PDI molecules in thin PMA films at a

dx.doi.org/10.1021/mz3002269 | ACS Macro Lett. 2012, 1, 784−788

temperature corresponding to T_g + 13 K. It has been shown before that the reorientation dynamics of a single dye molecule doped into a polymer film directly reflects the polymer relaxation process[25] even though it does not provide the same relaxation time values.[27] This is in agreement with results from ensemble methods which established long ago that dye reorientation in polymer melts or glasses provides information about the segmental motion of the polymer.[35−37] Here we found that in thin PMA films the relaxation time does not depend on the film thickness between 20 and 110 nm. In each film there is a high mobility layer at the surface with a thickness of less than 5 nm which is independent of the total film thickness. There is also possibly an immobile layer of less than 5 nm at the interface with the substrate. The relaxation times within the films do not depend on the position across the film thickness, and we observed no gradient in the relaxation process going from the surface to the substrate. These results which are schematically shown in Figure 3b should be viewed in the context of reports on thickness-dependent relaxation processes. It has been found for supported PS[9] and poly(methyl methacrylate) (PMMA)[10] films that the glass transition or the related relaxation processes change gradually from the surface (or substrate) into the film interior and that this gradual change can span lengths of tens of nanometers. Gradients in T_g on similar scales have been found also for free-standing PS films.[11] The results of a recent single-molecule diffusion study in supported PS films well above the T_g were also interpreted in terms of a gradient in glass transition across the film.[21] In comparison, our results on supported PMA films indicate a very thin surface (and possibly interface) layers with an abrupt change of dynamics between these layers and the bulk of the thin film. Mapping of local dynamics across thin films by monitoring reorientation and spatial diffusion of single dye molecules is a potentially direct and powerful tool to study polymer relaxation processes. Further experiments on temperature dependence of the relaxation which would include localization of molecules that started reorientation motion at particular temperature will help to obtain more information on the surface and interface regions and explain some of the above controversies.

■ ASSOCIATED CONTENT

Supporting Information

Experimental procedure for determining the axial z-position by astigmatic imaging of single molecules; histograms of coefficients β. This material is available free of charge via the Internet at http://pubs.acs.org.

■ AUTHOR INFORMATION

Corresponding Author

*E-mail: vacha.m.aa@m.titech.ac.jp.

Notes

The authors declare no competing financial interest.

■ ACKNOWLEDGMENTS

The authors thank Dr. Satoshi Habuchi (currently at KAUST, Saudi Arabia) for many helpful discussions. This work was supported by a Grant-in-Aid for Scientific Research No. 23651107 of the Japan Society for the Promotion of Science and by a Research Grant of Ogasawara Foundation.

■ REFERENCES

(1) Keddie, J. L.; Jones, R. A. L.; Cory, R. A. *Europhys. Lett.* **1994**, *27*, 59−64.
(2) Keddie, J. L.; Jones, R. A. L.; Cory, R. A. *Faraday Discuss.* **1994**, *98*, 219−230.
(3) Forrest, J. A.; Dalnoki-Veress, K.; Stevens, J. R.; Dutcher, J. R. *Phys. Rev. Lett.* **1996**, *77*, 2002−2005.
(4) Forrest, J. A.; Dalnoki-Veress, K.; Dutcher, J. R. *Phys. Rev. E* **1997**, *56*, 5705−5716.
(5) Aharoni, S. M. *Polym. Adv. Technol.* **1998**, *9*, 169−201.
(6) Alcoutlabi, M.; McKenna, G. B. *J. Phys.: Condens. Matter* **2005**, *17*, R461−R524.
(7) Tseng, K. C.; Turro, N. J.; Durning, C. J. *Phys. Rev. E* **2000**, *61*, 1800−1811.
(8) Yang, Z.; Fujii, Y.; Lee, F. K.; Lam, C.-H.; Tsui, O. K. C. *Science* **2010**, *328*, 1676−1679.
(9) Ellison, C. J.; Torkelson, J. M. *Nat. Mater.* **2003**, *2*, 695−700.
(10) Priestley, R. D.; Ellison, C. J.; Broadbelt, L. J.; Torkelson, J. M. *Science* **2005**, *309*, 456−459.
(11) Kim, S.; Torkelson, J. M. *Macromolecules* **2011**, *44*, 4546−4553.
(12) Peter, S.; Meyer, H.; Baschnagel, J.; Seemann, R. *J. Phys.: Condens. Matter* **2007**, *19*, 205119.
(13) Paeng, K.; Swallen, S. F.; Ediger, M. D. *J. Am. Chem. Soc.* **2011**, *133*, 8444−8447.
(14) Tress, M.; Erber, M.; Mapesa, E. U.; Huth, H.; Muller, J.; Serghei, A.; Schick, C.; Eichhorn, K. J.; Volt, B.; Kremer, F. *Macromolecules* **2010**, *43*, 9937−9944.
(15) Efremov, M. Y.; Olson, E. A.; Zhang, M.; Zhang, Z.; Allen, L. H. *Phys. Rev. Lett.* **2003**, *91*, 085703.
(16) Kajiyama, T.; Tanaka, K.; Takahara, A. *Macromolecules* **1997**, *30*, 280−285.
(17) Wöll, D.; Braeken, E.; Deres, A.; De Schryver, F. C.; Uji-i, H.; Hofkens, J. *Chem. Soc. Rev.* **2009**, *38*, 313−328.
(18) Kulzer, F.; Xia, T.; Orrit, M. *Angew. Chem., Int. Ed.* **2010**, *49*, 854−866.
(19) Vacha, M.; Habuchi, S. *NPG Asia Mater.* **2010**, *2*, 134−142.
(20) Habuchi, S.; Sato, N.; Yamamoto, T.; Tezuka, Y.; Vacha, M. *Angew. Chem., Int. Ed.* **2010**, *49*, 1418−1421.
(21) Flier, B. I.; Baier, M. C.; Huber, J.; Muellen, K.; Mecking, S.; Zumbusch, A.; Wöll, D. *J. Am. Chem. Soc.* **2012**, *134*, 480−488.
(22) Deschenes, L. A.; Bout, D. A. V. *J. Phys. Chem. B* **2002**, *106*, 11438−11445.
(23) Zondervan, R.; Kulzer, F.; Berkhout, G. C. G.; Orrit, M. *Proc. Natl. Acad. Sci. U.S.A.* **2007**, *104*, 12628−12633.
(24) Schob, A.; Cichos, F.; Schuster, J.; von Borczyskowski, C. *Eur. Polym. J.* **2004**, *40*, 1019−1026.
(25) Adhikari, S.; Selmke, M.; Cichos, F. *Phys. Chem. Chem. Phys.* **2011**, *13*, 1849−1856.
(26) Uji-i, H.; Melnikov, S. M.; Deres, A.; Bergamini, G.; De Schryver, F.; Herrmann, A.; Muellen, K.; Enderlein, J.; Hofkens, J. *Polymer* **2006**, *47*, 2511−2518.
(27) Deres, A.; Floudas, G. A.; Muellen, K.; Van der Auweraer, M.; De Schryver, F.; Enderlein, J.; Uji-i, H.; Hofkens, J. *Macromolecules* **2011**, *44*, 9703−9709.
(28) Hinze, G.; Basche, T.; Vallee, R. A. L. *Phys. Chem. Chem. Phys.* **2011**, *13*, 1813−1818.
(29) Mackowiak, S. A.; Leone, L. M.; Kaufman, L. J. *Phys. Chem. Chem. Phys.* **2011**, *13*, 1786−1799.
(30) Zheng, Z.; Kuang, F.; Zhao, J. *Macromolecules* **2010**, *43*, 3165−3168.
(31) Tomczak, N.; Vallée, R. A. L.; Van Dijk, E. M.; Kuipers, L.; Van Hulst, N. F.; Vancso, G. J. *J. Am. Chem. Soc.* **2004**, *126*, 4748−4749.
(32) Huang, B.; Wang, W.; Bates, M.; Zhuang, X. *Science* **2008**, *319*, 810−813.
(33) Badieirostami, M.; Lew, M. D.; Thompson, M. A.; Moerner, W. E. *Appl. Phys. Lett.* **2010**, *97*, 161103.
(34) Biteen, J. S.; Goley, E. D.; Shapiro, L.; Moerner, W. E. *ChemPhysChem* **2012**, *13*, 1007−1012.
(35) Ediger, M. D. *Annu. Rev. Phys. Chem.* **1991**, *42*, 225−250.

(36) Dhinojwala, A.; Wong, G. K.; Torkelson, J. M. *J. Chem. Phys.* **1994**, *100*, 6046−6054.
(37) Inoue, T.; Cicerone, M. T.; Ediger, M. D. *Macromolecules* **1995**, *28*, 3425−3433.